

Accepted Manuscript

Does sunspot numbers cause global temperatures? A reconsideration using non-parametric causality tests

Hossein Hassani, Xu Huang, Rangan Gupta, Mansi Ghodsi

PII: S0378-4371(16)30135-2

DOI: <http://dx.doi.org/10.1016/j.physa.2016.04.013>

Reference: PHYSA 17093

To appear in: *Physica A*

Received date: 9 January 2016

Revised date: 9 March 2016

Please cite this article as: H. Hassani, X. Huang, R. Gupta, M. Ghodsi, Does sunspot numbers cause global temperatures? A reconsideration using non-parametric causality tests, *Physica A* (2016), <http://dx.doi.org/10.1016/j.physa.2016.04.013>

This is a PDF file of an unedited manuscript that has been accepted for publication. As a service to our customers we are providing this early version of the manuscript. The manuscript will undergo copyediting, typesetting, and review of the resulting proof before it is published in its final form. Please note that during the production process errors may be discovered which could affect the content, and all legal disclaimers that apply to the journal pertain.



1
2
3
4
5
6
7
8
9
10
11
12
13
14
15
16
17
18
19
20
21
22
23
24
25
26
27
28
29
30
31
32
33
34

Does Sunspot Numbers Cause Global Temperatures? A Reconsideration Using Non-parametric Causality Tests*

Hossein Hassani¹, Xu Huang², Rangan Gupta³, Mansi Ghodsi¹

- 1- Institute for International Energy Studies (IIES), Tehran 1967743 711, Iran
- 2- The Statistical research Centre, Bournemouth University, UK
- 3- Department of Economics, University of Pretoria, Pretoria, 0002, South Africa

ABSTRACT

In a recent paper, Gupta et al., (2015), analyzed whether sunspot numbers cause global temperatures based on monthly data covering the period 1880:1-2013:9. The authors find that standard time domain Granger causality test fails to reject the null hypothesis that sunspot numbers does not cause global temperatures for both full and sub-samples, namely 1880:1-1936:2, 1936:3-1986:11 and 1986:12-2013:9 (identified based on tests of structural breaks). However, frequency domain causality test detects predictability for the full-sample at short (2 to 2.6 months) cycle lengths, but not the sub-samples. But since, full-sample causality cannot be relied upon due to structural breaks, Gupta et al., (2015) concludes that the evidence of causality running from sunspot numbers to global temperatures is weak and inconclusive. Given the importance of the issue of global warming, our current paper aims to revisit this issue of whether sunspot numbers cause global temperatures, using the same data set and sub-samples used by Gupta et al., (2015), based on a nonparametric Singular Spectrum Analysis (SSA)-based causality test. Based on this test, we however, show that sunspot numbers have predictive ability for global temperatures for the three sub-samples, over and above the full-sample. Thus, generally speaking, our non-parametric SSA-based causality test outperformed both time domain and frequency domain causality tests and highlighted that sunspot numbers have always been important in predicting global temperatures.

Keywords: Causality; Singular Spectrum Analysis; frequency domain; global temperatures predictability; sunspot numbers

JEL classification: C32

* We would like to thank two anonymous referees for many comments. However, any remaining errors are solely ours.

35 1. Introduction

36

37 Global warming, i.e., rising temperature of the earth's surface, is undoubtedly the biggest topic of
38 research amongst researchers working on environment. While, analyzing the impact of global
39 warming cannot be ignored, but what factors drive it is perhaps more important, as it not only allows
40 us to predict global warming, but also takes measures to control it. It is quite well-accepted that
41 global warming is due to greenhouse gases, additionally, there is a large literature¹ that relates the
42 same with solar activity. However, the evidence from this literature is, at best, mixed. While there
43 are studies (see for example, Lean and Rind, 1998, 2009; Scafetta and West, 2003, 2005; Scafetta et
44 al., 2004; Scafetta, 2009, 2011; Folland et al., 2013; Zhou and Tung, 2013) that find significant
45 relationships between solar radiation and global temperatures, one hand. On the other hand, there are
46 some authors who claim that the two variables are unrelated (see for example, Pittock, 1978, 1983,
47 2009; Love et al., 2011; Usoskin, et al., 2004). Thus, there is no clear-cut consensus about the
48 possibility of a relationship between solar irradiance and global temperatures (Gil-Alana et al.,
49 2014).

50 Against this backdrop, using sunspot numbers as a proxy for solar activity, Gupta et al.,
51 (2015), recently analyzed whether sunspot numbers cause global temperatures based on monthly data
52 covering the period 1880:1-2013:9. However, at this stage, it is important to point out, as indicated
53 by Scafetta (2014), sunspot numbers can only be considered as a "partial proxy" for solar activity.
54 This is because time intervals between major solar flares, cosmic ray records, ACRIM composite of
55 total solar irradiance satellite measurement, multi-scale thermal models of several total solar
56 irradiances, and solar and astronomical oscillations are also possible, and perhaps, better proxies for
57 solar activity than sunspot numbers. In addition, one must be cautious in suggesting that sunspot
58 numbers are linearly and positively related to solar activity due to the intrinsic complexity of solar

¹ The reader is referred to Gray et al. (2010) and Gupta et al., (2015) for further details.

59 dynamics and of its multiple coupled phenomena, as discussed in detail in Scafetta (2014). Gupta et
60 al., (2015) find that standard time domain Granger causality test fails to reject the null hypothesis
61 that sunspot numbers does not cause global temperatures for both full and sub-samples, namely
62 1880:1-1936:2, 1936:3-1986:11 and 1986:12-2013:9 (identified based on tests of structural breaks).
63 However, frequency domain causality test detects predictability for the full-sample at short (2 to 2.6
64 months) cycle lengths. Interestingly however, the study could not detect any causality for the sub-
65 samples. Gupta et al., (2015) thus, highlights the importance of analysing causality using the
66 frequency domain tests, which, unlike the time domain Granger causality test, allows one to
67 decompose causality by different time horizons, and hence, possibly detect predictability at certain
68 cycle lengths even when the time domain causality test might fail to pick up any causality. However,
69 given that there exists structural breaks in the sample, Gupta et al., (2015), suggests that the
70 relationship could be spurious based on a full-sample analysis, since a full-sample analysis assumes
71 stability of the parameters of a VAR, which is clearly not the case in the presence of breaks, and
72 which is also vindicated by the fact that there is no evidence of causality over the sub-samples.

73 Given the importance of the issue of global warming, and more importantly the lack of
74 evidence in favor of sunspot numbers leading to global temperatures in linear models, our current
75 paper aims to revisit this issue of whether sunspot numbers cause global temperatures, using the
76 same data set and sub-samples used by Gupta et al., (2015), based on Singular Spectrum Analysis
77 (SSA) technique, which is a new nonparametric technique known for both time series analysis and
78 forecasting (as discussed further in Hassani, 2007; Hassani and Thomakos, 2010; Hassani et al., 2009,
79 2010, 2013a, 2013b; Hassani and Mahmoudvand, 2013). The reason behind using a nonparametric
80 technique is to capture possible nonlinearities that could exist in the data generating processes of the
81 global temperatures and sunspots individually (Scafetta, 2014), as well as, in the relationship
82 between global temperatures and sunspot activity, for instance due to the structural breaks detected

83 by Gupta et al., (2015). The SSA being a nonparametric method captures the possible nonlinearities
84 using a data-driven approach, without specifying any known functional nonlinear model to the
85 relationship, which in turn, could be incorrectly specified in the first place, just like the linear model,
86 on which time domain and frequency domain Granger causality tests are based on. Further, as
87 pointed out by Aguirre et al., (2008), the difficulties encountered in modeling sunspot numbers and
88 global temperature data are due to the apparent nonstationarity property of the series and the
89 complex dynamic fluctuations in the cycle amplitude of the sunspot number series. In other words,
90 these complexities could be driving the mixed results discussed above in terms of the relationship
91 between these two variables. In light of this, the importance of the nonparametric SSA-based
92 causality cannot be underestimated, which besides being a nonlinear data-driven approach, also does
93 not require pretesting to ensure that the variables under consideration is stationary (Hassani, 2007;
94 Hassani and Thomakos, 2010; Hassani et al., 2009, 2010, 2013a, 2013b; Hassani and Mahmoudvand,
95 2013).

96 The paper is structured as follows: Given that time and frequency domain causality tests were
97 already discussed in Gupta et al., (2015), the details of the frequency domain causality test have been
98 relegated to the appendix for the sake of completeness, with Section 2 introducing the SSA-based
99 causality test (following the works of Hassani and Mahmoudvand, 2013). Section 3 presents the data
100 and empirical results. Finally, Section 4 concludes.

101

102 **2. Methodology: The SSA-based causality test (MSSA)**

103

104 Multivariate singular spectrum analysis (MSSA) is an extension of the standard Singular Spectrum
105 Analysis (SSA) to the case of multivariate time series (Hassani et al., 2013), in which SSA is a
106 relatively new nonparametric technique known for both time series analysis and forecasting, detail
107 description can be found in (Hassani, 2007). After Broomhead and King (1986) theoretically

108 proposed the MSSA technique in the context of nonlinear dynamics for the first time, it has been
 109 widely applied on a range of different fields and a multitude of fairly precise results proved it as
 110 powerful and applicable technique, numerous applications and examples can be found in (Hassani,
 111 2007; Hassani et al., 2009, 2010, 2013a, 2013b; Ghodsi et al., 2010; Hassani and Thomakos, 2010;
 112 Hassani and Mahmoudvand, 2013; Sanei and Hassani, 2015). From the perspective of MSSA, two
 113 main concerns that make the problem more complex are: i) similarity and orthogonality among series
 114 play an important rule for selecting the window length L and the number of eigenvalues r , and ii)
 115 MSSA deals with a block trajectory Hankel matrix with special features rather than one simple
 116 Hankel matrix (Hassani and Mahmoudvand, 2013). Briefly descriptions of MSSA and causality
 117 criteria are listed in following subsections.

118

119 2.1 Algorithm Description of MSSA

120 In this subsection of brief description of MSSA algorithm, we mainly follow the paper by Hassani
 121 and Mahmoudvand (Hassani and Mahmoudvand, 2013). Consider M time series with different series
 122 length N_i as $Y_{N_i}^{(i)} = (y_1^{(i)}, \dots, y_{N_i}^{(i)}) (i = 1, \dots, M)$. By the embedding process that transfer a one-
 123 dimensional series $Y_{N_i}^{(i)} = (y_1^{(i)}, \dots, y_{N_i}^{(i)})$ in to a multidimensional matrix $[X_1^{(i)}, \dots, X_{K_i}^{(i)}]$ with
 124 vectors $X_j^{(i)} = (y_j^{(i)}, \dots, y_{i+L_j-1}^{(i)})^T \in R^{L_i}$, where $L_i (2 \leq L_i \leq N_i)$ is the window length for each series
 125 with length N_i and $K_i = N_i - L_i + 1$. We can then get the trajectory matrix $X^{(i)} = [X_1^{(i)}, \dots, X_{K_i}^{(i)}] =$
 126 $(x_{mn})_{m,n=1}^{L_i, K_i}$ after this step. The above procedure for each series separately provides M different
 127 $L_i \times K_i$ trajectory matrices $X^{(i)} (i = 1, \dots, M)$. To construct a block Hankel matrix, we need to
 128 have $L_1 = L_2 = \dots = L_M = L$. Therefore, we have different values of K_i and series length N_i , but
 129 similar L_i . The result of this step is $X_H = [X^{(1)}: X^{(2)}: \dots: X^{(M)}]$. Hence, the structure of the matrix

130 $X_H X_H^T$ is as follows: $X_H X_H^T = X^{(1)} X^{(1)T} + \dots + X^{(M)} X^{(M)T}$ and the sum of $X^{(i)} X^{(i)T}$ provides the new
 131 block Hankel matrix, which can be subsequently converted to a time series.

132

133 2.2 Causality criteria based on forecasting accuracy

134 Granger (1969) proposed and formalized the causality concept to address the question that whether
 135 one variable can help in predicting another. The criterion we use is based on out-of-sample
 136 forecasting, which is very common in the framework of Granger causality. Here, we compare the
 137 forecast values obtained by the univariate procedure, SSA and MSSA. If the forecasting errors using
 138 MSSA are significantly smaller than those of univariate SSA, we can conclude that there is a causal
 139 relationship between these series. Brief introduction is listed below which we mainly follow Hassani
 140 et al. (2010)².

141 Let us consider the procedure for constructing vectors of forecasting error for out-of-sample
 142 tests in a two variable case X_T and Y_T by both univariate and multivariate SSA techniques
 143 respectively. In the first step we divide the series $X_T = (x_1, \dots, x_T)$ into two separate subseries X_R
 144 and X_F : $X_T = (X_R, X_F)$, where $X_R = (x_1, \dots, x_R)$ and $X_F = (x_{R+1}, \dots, x_T)$. Same procedure is
 145 conducted for Y_T . The subseries X_R and Y_R are used in the reconstruction step to provide the noise-
 146 free series \tilde{X}_R and \tilde{Y}_R . The noise-free series are then used for forecasting the subseries X_F and Y_F with
 147 the help of the recursive formula using SSA and MSSA respectively. For variable X_T , two different
 148 forecasting values of $\hat{X}_F = (\hat{x}_{R+1}, \dots, \hat{x}_T)$ by SSA and MSSA are then used for computing the
 149 forecasting errors accordingly, which will be the same process for variable Y_T . Therefore, in a
 150 multivariate system like this, the vectors of forecasts obtained can be used in computing the
 151 forecasting accuracy and therefore examining the association between the two variables.

² The readers are referred to Hassani et al. (2010) for more details.

152 The length of out-of-sample does not have specific limitation, generally considering the
153 simulation scenario, the length of time series for reconstruction will take 2/3 of the whole series and
154 the rest 1/3 is considered as out-of-sample for constructing forecasting error. The separate point to
155 define the out-of-sample size for different series can be chosen respectively, whilst it is important
156 that when it goes to comparing the performances of different techniques based on constructed
157 forecasting error of one specific series, the sizes of reconstruction and out-of-sample for all
158 techniques should be identical. In addition, the choices of window length L and the referring options
159 of numbers of eigenvalues r should also be carefully evaluated in practice of SSA-based causality
160 test respectively. In order to conduct the most accurate causality detection results, all the possibilities
161 of L and its referring choices of r should be applied for both univariate SSA and MSSA processes,
162 then the optimal ones with best performance of forecasting will be chosen to construct the finally
163 causality detection procedure.

164 Therefore, here we define the criterion $F_{X|Y} = \Delta X_F|Y / \Delta X_F$ corresponding to the forecast of
165 the series X_T in the presence of the series Y_T . If $F_{X|Y}$ is small, then having information obtained from
166 the series Y can help us to have better forecasts of the series X . If $F_{X|Y} < 1$, we conclude that the
167 information provided by the series Y can be regarded as useful or supportive for forecasting the
168 series X . Alternatively, if the values of $F_{X|Y} \geq 1$, then either there is no detectable association
169 between X and Y or the performance of the univariate SSA is better than of the MSSA (this may
170 happen, for example, when the series Y has structural breaks misdirecting the forecasts of X).

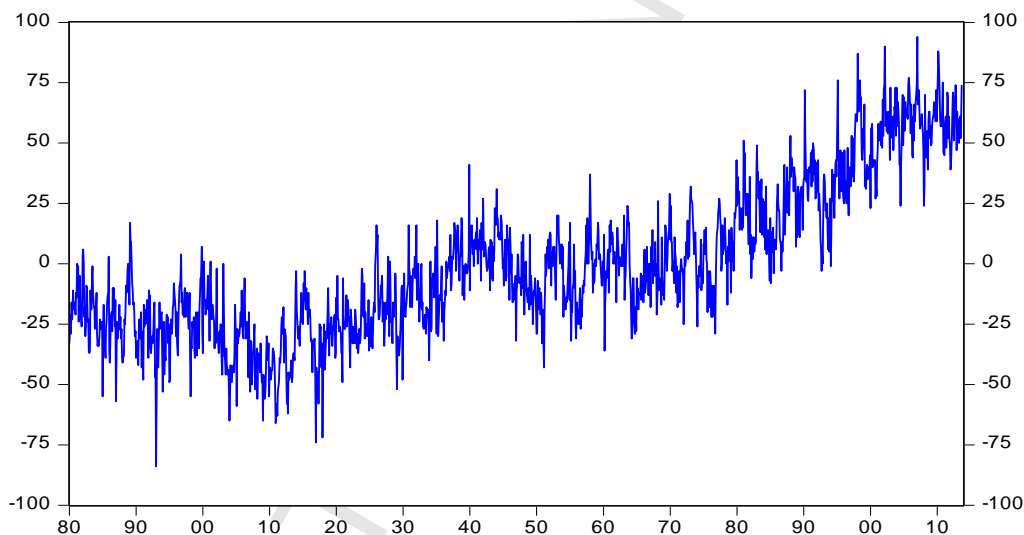
171

172 3. Data and empirical results

173

174 The data are at monthly frequency for global land-ocean temperatures (GT) and sunspot numbers
175 (SS), and cover the period from January 1880 to September 2013, with the start and end-points being

176 maintained the same as that of Gupta et al., (2015) for the sake of comparison. Empirical results, for
177 the time-domain causality and the SSA tests listed in this section are conducted by R programming
178 based on source code, while the frequency domain causality tests are performed in GAUSS. In terms
179 of the data, the global temperatures were obtained from the National Aeronautics and Space
180 Administration's (NASA), Goddard Institute for Studies (GISS) (<http://data.giss.nasa.gov/gistemp>),
181 while the sunspot numbers were obtained from the Solar Influences Data Analysis Centre (SIDC:
182 <http://www.sidc.be/sunspot-data>). The data for temperatures are anomalies relative to the base period
183 1951-1980. Figures 1(a) and 1(b) plot the two variables. As can be seen, the plot of the global
184 temperature seems to be non-stationary, though it could well be trend-stationary, while that of the
185 sunspot looks stationary with a cyclical pattern completed at about 10/11 years.



186
187 **Figure 1(a): Plot of Global Temperatures (1880:1-2013:9)**

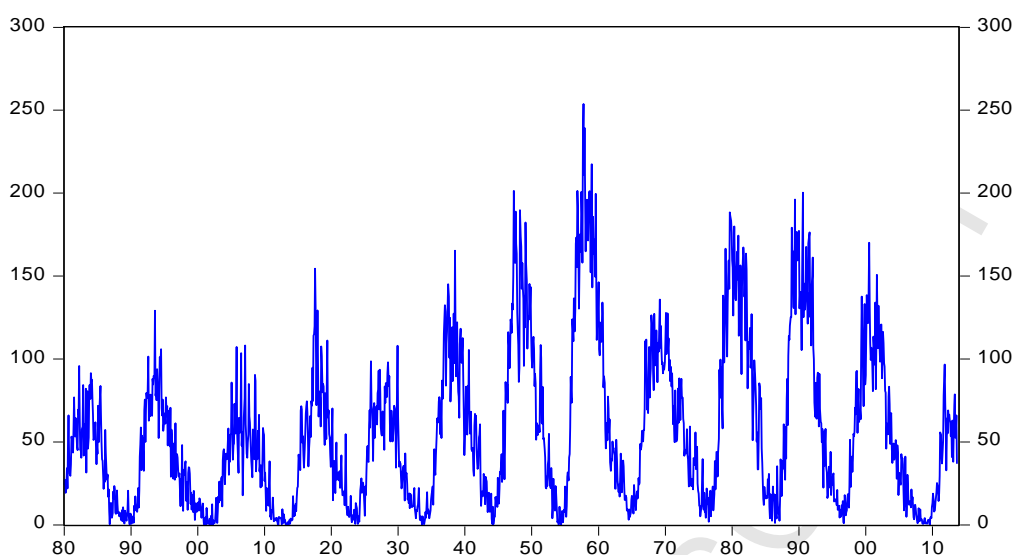


Figure 1(b): Plot of Sunspot Numbers (1880:1-2013:9)

188

189

190

191

192

193

194

195

196

197

198

199

200

201

202

203

204

As in Gupta et al., (2015), we start off with unit root tests to verify whether the two series are stationary $I(0)$ or not. As can be seen, based on the Kwiatkowski-Phillips-Schmidt-Shin (1992, KPSS), augmented Dickey-Fuller (1981, ADF), Dickey-Fuller test with Generalised least Squares detrended residuals (Elliot et al., 1996, DF-GLS) Phillips and Perron (1988, PP), and Ng and Perron (2001, NP) unit root tests, the null of a unit root is overwhelmingly rejected (except for KPSS test the null of being stationary, it cannot be overwhelmingly rejected), for the total sample of SS. However, for total sample of GT, while all the tests support that the variable is trend-stationary, the ADF and DF-GLS test tends to suggest non-stationarity of the series when the unit root test-equation has only a constant (or neither a constant and trend in case of the ADF test). The PP and the NP tests, though, indicate stationarity even under the assumption of constant only (and neither a constant and trend in case of the PP test).

As Gupta et al., (2015) points out, among the unit root tests conducted, the NP test is believed to have overwhelmingly stronger power relative to the other tests, and hence, one would tend to rely on the results from this test. Also, given the nature of GT, it is evident that the unit root equation

205 should in fact include a trend, while that for SS, it should only be with a constant. In light of this as
 206 in Gupta et al., (2015), we can conclude that GT is stationary as well, and hence, we do not need to
 207 transform the data further for either GT or SS. In addition, we do not need to account for the
 208 possibility cointegration, and hence error-correction, between the two variables.

209 Note that Gupta et al., (2015) applied Bai and Perron's (2003) sequential and repartition tests
 210 of multiple structural breaks on the GT equation of the VAR (4) model comprising of GT and SS.
 211 The GT equation on which the tests were performed involved a constant and four lags each of GT
 212 and SS. Now since structural breaks were detected in the full-sample at 1936:3 and 1986:12, we also
 213 conducted the unit root tests over the sub-samples, which are reported in Table 1. In general, for
 214 subsample A and subsample B we have overwhelming evidence of stationary (especially based on
 215 the results of NP test, which mentioned above that have stronger power compared to the other tests).
 216 For sample C, while GT is found to be stationary in general, the evidence of stationarity,
 217 surprisingly, is quite weak for SS, barring the PP and NP tests, at 10 % level of significance. But
 218 given the cyclical pattern of SS, it is very difficult to believe that the variable is non-stationary. In
 219 fact, we can conclude that the variable is weakly stationary for sub-sample C. In summary, for the
 220 full sample and all sub-samples, both variables are stationary.

221

222

Table 1: Unit Root Test Results

Sample Size	Series	Methods	None		Intercept		Intercept and Trend	
			Level	Decision	Level	Decision	Level	Decision
Total Sample (1605 Obs) 1880:1-2013:9	GT	KPSS	-----	-----	4.136*** (31)	I(1)	0.638***(30)	I(1)
		ADF	-1.620 (17)	I(1)	-1.598 (17)	I(1)	-3.707** (24)	I(0)
		PP	-6.231*** (12)	I(0)	-6.222*** (12)	I(0)	-18.761*** (23)	I(0)
		DF-GLS	-----	-----	-1.539 (6)	I(1)	-6.868*** (3)	I(0)
		NP	-----	-----	-33.684*** (12)	I(0)	-537.250*** (23)	I(0)
	SS	KPSS	-----	-----	0.494** (31)	I(1)	0.119 (31)	I(0)
		ADF	-2.499** (3)	I(0)	-4.055*** (3)	I(0)	-4.109*** (3)	I(0)
		PP	-3.457*** (13)	I(0)	-6.488*** (12)	I(0)	-6.800*** (13)	I(0)

		DF-GLS	-----	-----	-3.303***(3)	I(0)	-4.029***(3)	I(0)
		NP	-----	-----	-52.985***(12)	I(0)	-81.5259***(13)	I(0)
Subsample A (674 Obs) 1880:1-1936:2	GT	KPSS	-----	-----	0.455*(19)	I(1)	0.430***(19)	I(0)
		ADF	-2.710***(3)	I(0)	-7.207***(2)	I(0)	-7.228***(2)	I(0)
		PP	-4.313***(2)	I(0)	-13.397***(14)	I(0)	-13.424***(14)	I(0)
		DF-GLS	-----	-----	-6.325***(2)	I(0)	-7.076***(2)	I(0)
		NP	-----	-----	-234.149***(14)	I(0)	-275.304***(14)	I(0)
	SS	KPSS	-----	-----	0.053(21)	I(0)	0.051(21)	I(0)
		ADF	-1.819*(3)	I(1)	-3.451***(3)	I(0)	-3.447**(3)	I(0)
		PP	-3.226***(18)	I(0)	-6.075***(8)	I(0)	-6.075***(8)	I(0)
		DF-GLS	-----	-----	-3.043***(3)	I(0)	-3.322**(3)	I(0)
		NP	-----	-----	-52.499***(8)	I(0)	-57.985***(8)	I(0)
Subsample B (609 Obs) 1936:3-1986:11	GT	KPSS	-----	-----	0.794***(17)	I(1)	0.321***(16)	I(1)
		ADF	-7.121***(1)	I(0)	-7.211***(1)	I(0)	-7.515***(1)	I(0)
		PP	-12.979***(13)	I(0)	-13.102***(13)	I(0)	-13.678***(13)	I(0)
		DF-GLS	-----	-----	-3.287***(2)	I(0)	-6.454***(1)	I(0)
		NP	-----	-----	-92.270***(13)	I(0)	-229.775***(13)	I(0)
	SS	KPSS	-----	-----	0.061(18)	I(0)	0.052(18)	I(0)
		ADF	-1.690*(2)	I(1)	-2.720*(2)	I(1)	-2.741(2)	I(1)
		PP	-1.932*(11)	I(1)	-3.600***(2)	I(0)	-3.614**(2)	I(0)
		DF-GLS	-----	-----	-2.718***(2)	I(0)	-2.754*(2)	I(1)
		NP	-----	-----	-24.056***(2)	I(0)	-24.089***(2)	I(0)
Subsample C (322 Obs) 1986:12-2013:9	GT	KPSS	-----	-----	1.651***(14)	I(1)	0.126*(12)	I(0)
		ADF	-0.682 (3)	I(1)	-4.604***(1)	I(0)	-6.618***(1)	I(0)
		PP	-1.203 (26)	I(1)	-6.835***(8)	I(0)	-9.997***(8)	I(0)
		DF-GLS	-----	-----	-1.178*(3)	I(1)	-5.614***(1)	I(0)
		NP	-----	-----	-16.711***(8)	I(0)	-106.142***(8)	I(0)
	SS	KPSS	-----	-----	0.534**(15)	I(1)	0.093 (14)	I(0)
		ADF	-0.936 (3)	I(1)	-1.812 (3)	I(1)	-2.415 (3)	I(1)
		PP	-1.497(12)	I(1)	-2.761*(2)	I(0)	-3.394*(2)	I(0)
		DF-GLS	-----	-----	-1.138(3)	I(1)	-1.356(3)	I(1)
		NP	-----	-----	-6.718*(2)	I(0)	-8.802(2)	I(1)

223 Notes: **, * and *** indicates significance at the 10%, 5% and 1% level, respectively. The critical values are as follows:

- 224 - None: -2.566, -1.941 and -1.616 for ADF and PP at 1%, 5% and 10% level of significance, respectively.
- 225 - Intercept: -3.434, -2.863 and -2.567 (-2.566, 1.941, 1.617) [-13.8, -8.1 and -5.7] {0.739, 0.463, 0.347} for ADF
- 226 and PP (DF-GLS) [NP] {KPSS} at 1%, 5% and 10% level of significance, respectively.
- 227 - Intercept and Trend: -3.963, -3.412 and -3.128 (3.48, 2.89, 2.57) [-23.80, -17.3 and -14.2] {0.216, 0.146, 0.119}
- 228 for ADF and PP (DF-GLS) [NP] {KPSS} at 1%, 5% and 10% level of significance, respectively.
- 229 Numbers in parentheses for ADF, PP and DF-GLS tests indicates lag-lengths selected based on the Schwarz Information
- 230 Criterion (SIC). For the NP test and the KPSS test, based on the Bartlett kernel spectral estimation method, the
- 231 corresponding numbers are the Newey-West bandwidth.

232
233

234 Though our primary interest is to analyze causality between global temperatures and sunspot
 235 numbers using the SSA approach, for the sake of completeness, we also present here the results in
 236 time and frequency domains, as used in Gupta et al., (2015).

237 As shown in Table 2 the null hypothesis that SS does not Granger cause GT cannot be
 238 rejected for both full and the sub-samples – a result also pointed out by Gupta et al., (2015). This
 239 result continues to hold when we also detrend GT.^{3,4}

240 **Table 2. Time-Domain Granger Causality Test Results**

241

Sample and Number of Observation		Total Sample (1605 Obs)		Subsample A (674 Obs)		Subsample B (609 Obs)		Subsample C (322 Obs)	
Referring Periods		1880:1-2013:9		1880:1-1936:2		1936:3-1986:11		1986:12-2013:9	
Causality Direction		SS-->GT		SS-->GT		SS-->GT		SS-->GT	
Tested Series	Original	F	p-value	F	p-value	F	p-value	F	p-value
		1.0107	0.3642	0.947	0.3884	1.1374	0.3213	1.5871	0.2062
	De-trended	F	p-value	F	p-value	F	p-value	F	p-value
		1.3569	0.2287	1.2343	0.2949	1.6907	0.1505	0.9201	0.4525

242

243 Next, we repeat and present the frequency domain causality results of Gupta et al., (2015) for
 244 the full and the sub-samples in Figures 2, with the same lag-structure as used in the time domain
 245 Granger causality tests. The figures depict the test statistics (solid line) along with their 5 percent
 246 critical values (broken line) for all frequencies in the interval $(0, \pi)$, to assess the predictive content
 247 of SS for GT. For the full-sample (1880:1-2013:9), the null hypothesis of non-predictability is
 248 rejected for ω greater than 2.45 corresponding to a cycle length between 2 and 2.6 months.⁵ For the
 249 sub-samples 1 (1880:1-1936:2), 2 (1936:3-1986:11) and 3 (1986:12-2013:9), however, the null of no

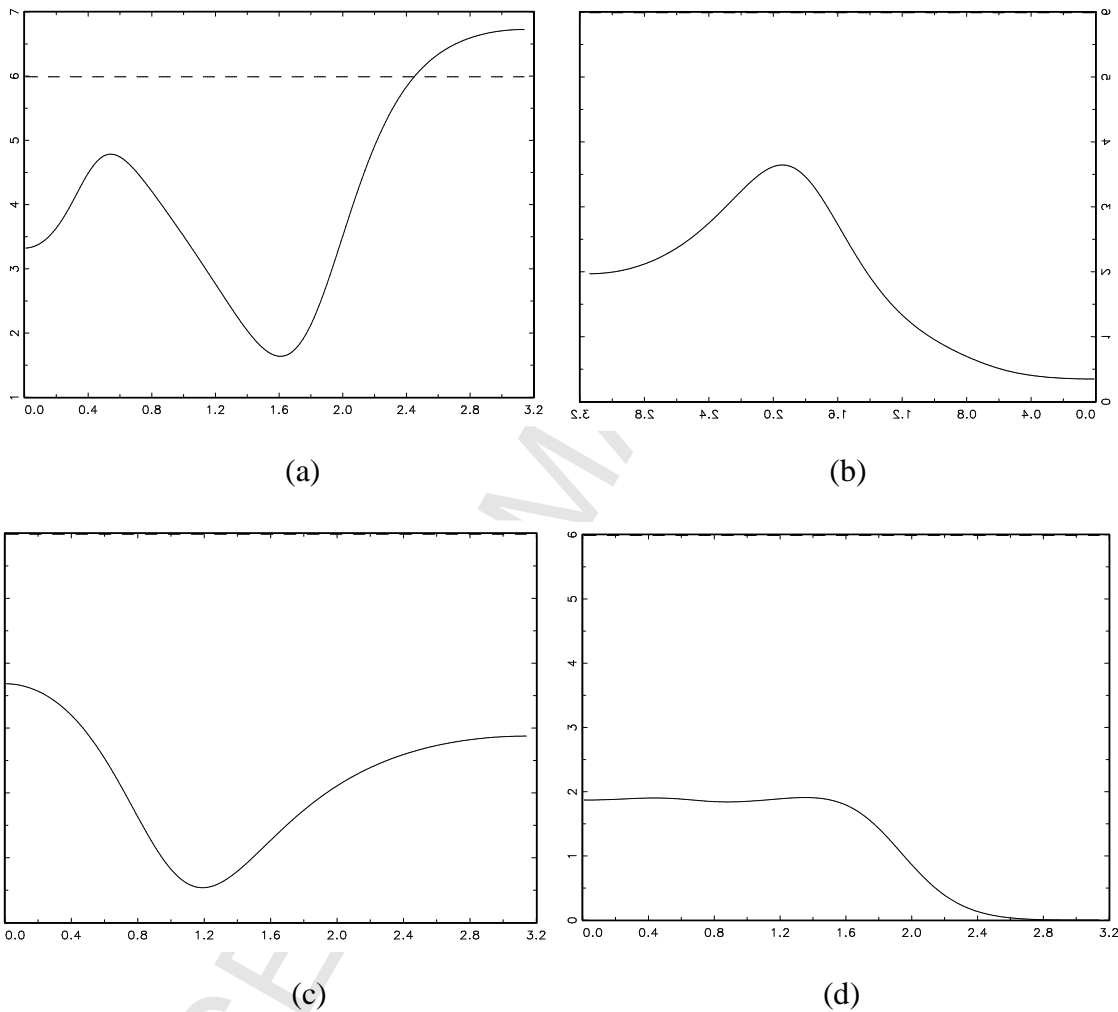
³ Given the weak evidence of stationarity for SS for sub-sample C, we repeated the Granger causality test with first differences of SS and GT without and with detrending. The null of non-causality still continued to hold with p -values of 0.7279 and 0.6597, respectively. Further details on these results are available upon request from the authors.

⁴ Based on the suggestions of an anonymous referee, we also conducted the nonparametric rank Granger causality tests which is robust to non-normal errors of Holmes and Hutton (1990). However, as with the standard Granger causality tests, the null of no-causality could not be rejected at the conventional 5 percent level of significance. Complete details of these results are available upon request from the authors.

⁵ Recall that, the frequency (ω) on the horizontal axis can be translated into a cycle or periodicity of T months by $T = (2\pi / \omega)$, where T is the period.

250 predictability cannot be rejected for any frequency. So, as in the time domain Granger causality tests
 251 for the sub-samples, the frequency domain tests too fail to reject the null that SS has no predictability
 252 for GT in the sub-samples. Since in the presence of structural breaks, the full-sample causality results
 253 cannot be relied upon, our frequency domain causality tests, as in Gupta et al., (2015), tend to
 254 suggest that there is no causality running from SS to GT

255



256

257

258

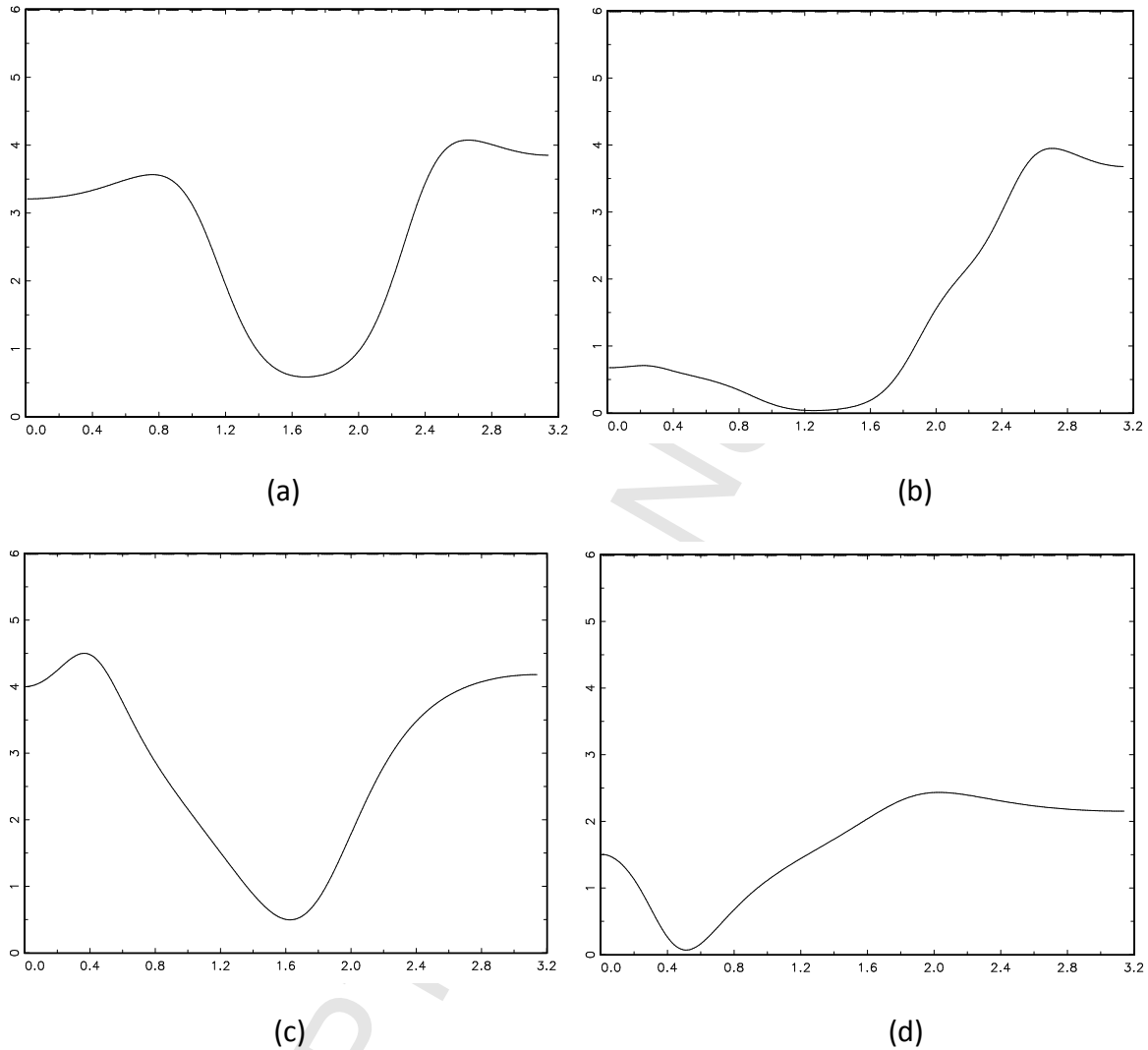
259

260 **Figure 2: Frequency Domain Causality of -- (a) Total Sample (1880:1-2013:9), (b) Subsample A**
 261 **(1880:1-1936:2), (c) Subsample B (1936:3-1986:11), (d) Subsample C (1986:12-2013:9).**

262

263 As with the time domain tests, we also present below, in Figures 3, the results from the
 264 frequency domain test of GT after detrending. As can be seen, now there is no evidence of causality

265 either for the full-sample or sub-samples any frequency. This result could imply that results based on
 266 trending GT series for the full-sample could have been spurious in the frequency domain as reported
 267 in Gupta et al., (2015).



268

269

270

271

272 **Figure 3: Frequency Domain Causality with Detrended GT of – (a) Total Sample (1880:1-**
 273 **2013:9), (b) Subsample A (1880:1-1936:2), (c) Subsample B (1936:3-1986:11), (d) Subsample C**
 274 **(1986:12-2013:9).**

275

276 Against this background of lack of evidence of causality in the time and frequency domains,
 277 we now next turn our attention to the causality using the SSA-based approach. As mentioned in 2.2,
 278 in order to conduct the SSA-based Causality Test for the sunspot and global temperature data, the

279 out-of-sample size for each subsample series is 1/3 of the whole series. In addition, before the last
280 step which determines causality by causality criterion $F_{GT|SS}$ in 2.2, all the forecasting results of both
281 SSA and MSSA steps are the optimal choice chosen respectively after considering all the
282 possibilities of window length L and its corresponding choices of number of eigenvalues r . The
283 following table summarizes the causality test results based on SSA technique. As what is mentioned
284 in 2.2, if the causality criterion $F_{GT|SS} \geq 1$, then either there is no detectable association between GT
285 and SS or the performance of the univariate SSA is better than of the MSSA, this may happen, for
286 example, when one of the series has structural breaks misdirecting the forecasts; If $F_{GT|SS} < 1$, then
287 we conclude that the information provided by the series Y can be regarded as useful or supportive for
288 forecasting the series X . According to the following table, when the whole sample is considered, the
289 test statistics is very close to 1 and could not provide strong information to determine the causality
290 between GT and SS . This is possibly affected by the structural breaks we detected in GT , which
291 misleads the forecasts. Comparing with the empirical evidence of Gupta et al., (2015), whereby the
292 authors detected causality only in for the full-sample, our SSA-based causality tests, provides strong
293 evidence of causality for all the-subsamples as well, to go on with the weak evidence of causality for
294 the full-sample. In addition, considering the detrended GT series in comparison with using the GT
295 with trend for our tests, the causality for all subsamples and the weak evidence for total samples still
296 hold. Recall, when we repeated the frequency domain analysis for Gupta et al., (2015) using
297 detrended GT , we could not detect causality even for the full-sample – a result also obtained for the
298 time-domain version of the test.⁶ In more details, subsample A show the strongest effect comparing
299 to other subsamples regardless of the original and de-trended series; followed by subsample C with
300 slightly weaker causal effect from SS to GT ; moreover, the weakest causal effect holds for
301 subsample B according to tests of both original and de-trended series.

⁶ For a discussion of causality based on cross-spectrum analysis between GT and SS , refer to the Appendix of this paper.

Table 3. SSA-based Causality Test Results

Sample and Number of Observation		Total Sample (1605 Obs)	Subsample A (674 Obs)	Subsample B (609 Obs)	Subsample C (322 Obs)
Referring Periods		1880:1-2013:9	1880:1-1936:2	1936:3-1986:11	1986:12-2013:9
Test Statistics		$F_{GT SS}$	$F_{GT SS}$	$F_{GT SS}$	$F_{GT SS}$
Series	Original	0.998	0.284	0.399	0.308
	De-trended	0.967	0.400	0.800	0.465

Note that $F_{GT|SS}$ is the criterion of SSA-based causality test based on forecasting accuracy (see 2.2).

4. Concluding remarks

Global warming is undoubtedly the biggest topic of research amongst researchers working on environment. What drives global temperatures is understandably an interesting area of research. While greenhouse gases emissions are believed to be a major cause, there is also a large literature that tends to suggest that solar activity also drives global temperatures. However, the evidence in terms of the latter line of reasoning is mixed. Given this, in a recent paper, Gupta et al., (2015) analyzed whether sunspot numbers cause global temperatures based on monthly data covering the period 1880:1-2013:9, using not only time-domain, but also frequency domain causality tests. The authors find that standard time domain Granger causality test fails to reject the null hypothesis that sunspot numbers does not cause global temperatures for both full and sub-samples, namely 1880:1-1936:2, 1936:3-1986:11 and 1986:12-2013:9 (identified based on tests of structural breaks). However, frequency domain causality test detects predictability for the full-sample at short (2 to 2.6 months) cycle lengths. As with the time domain results, no causality however, could be detected for the sub-samples. But since, full-sample causality cannot be relied upon due to structural breaks, as Granger causality tests assumes constancy of parameters during the sub-sample, which is of course not the case with structural breaks, Gupta et al., (2015) concludes that the evidence in favour of sunspot numbers causing global temperatures is weak, if not non-existent.

324 Given the importance of the issue of global warming, our current paper aims to revisit the
325 question of whether sunspot numbers cause global temperatures, using the same data set and sub-
326 samples used by Gupta et al., (2015), but now, based on an advanced new nonparametric technique --
327 the Singular Spectrum Analysis (SSA)-based causality test. Our nonparametric technique is able to
328 capture possible nonlinearities that could exist in the data generating processes of the global
329 temperatures and sunspots, but also, in the relationship between global temperatures and sunspot
330 activity, for instance due to the structural breaks. The SSA being a nonparametric method captures
331 the possible nonlinearities using a data-driven approach, without specifying any known functional
332 nonlinear model to the relationship, which in turn, could be incorrectly specified in the first place, as
333 is possibly the linear model. Using the SSA-based causality tests, we show that sunspot numbers
334 have predictive ability for global temperatures for the all three sub-samples, over and above the full-
335 sample, even if the latter result can be ignored due to structural instability. Thus, the non-parametric
336 SSA-based causality test outperforms both time domain and frequency domain causality tests, and,
337 more importantly, highlights that sunspot numbers have always been important in predicting global
338 temperatures. In other words, researchers working on global warming can predict movements of the
339 global temperatures based on movements in sunspot activity, but for this, they need to rely on a
340 nonlinear data-driven, i.e., nonparametric approach.

341 Given the importance global warming, two areas of future research would be: (1) Since
342 there is evidence of causality in the full-sample, it is clear that there must be causality at certain
343 specific points in time, even if it is not for the sub-samples identified based on structural breaks. In
344 light of this, one needs to undertake a time-varying or rolling sub-samples based test of causality.
345 Also, in this regard, it is important to analyze the direction or the sign of the effect of this causal
346 relationship if it exists at specific points in time, to design environmental policies better, and (2) Here
347 we analyze in-sample predictability, in the future it would be interesting to compare linear and

348 nonlinear models in forecasting out-of-sample global temperatures based on sunspot numbers. This
349 would provide information, ahead of time as to where global temperatures are headed given an
350 existing set of information on sunspot numbers.

351 Finally, as a cautionary note, it is important to highlight, something that we have touched
352 above as well, that the Earth's climate is regulated by anthropogenic emissions like CO₂, volcanoes
353 and other greenhouse gases, which need to be factored in as well to properly identify the contribution
354 of solar activity (Scafetta, 2014). Ignoring these issues could also lead to spurious, in other words,
355 more significant influence from sunspot numbers on global temperatures. However, in our case, the
356 objective was replicating the work of Gupta et al., (2015), and over the same sample period data on
357 CO₂ emissions were only available at annual frequency. In this regard, an interesting piece of recent
358 work can be found in Hassani et al., (2015). In addition, while we are only analyzing causality and
359 not correlation between sunspot numbers and global temperatures, we must be careful in saying that
360 sunspot numbers used as a partial proxy for solar activity are positively (and linearly), since this
361 might not be the case, and hence. In other words, our evidence of causality between sunspot numbers
362 and global temperatures should not be associated with positive correlation between these two
363 variables. The sign of this relationship is beyond the scope of this paper.

364

365

366

367

368

369

370

371

372

373

References

- 374 Aguirre, L.A., Letellier, C. and Maquet, J. (2008). Forecasting the time series of sunspot numbers.
 375 Solar Physics, 249, 103-120.
- 376
- 377 Bai, J. and Perron, P. (2003). Computation and analysis of multiple structural change models. Journal
 378 of Applied Econometrics, 18, 1-22.
- 379 Breitung, J. and Candelon, B. (2006). Testing for short- and long-run causality: A frequency-domain
 380 approach. Journal of Econometrics, 132, 363-378.
- 381
- 382 Broomhead, D.S. and King, G.P. (1986). Extracting qualitative dynamics from experimental data.
 383 Physica D: Nonlinear Phenomena, 20(2-3), 217-236.
- 384
- 385 Dickey, D. and Fuller, W. (1981). Likelihood ratio statistics for autoregressive time series with a unit
 386 root. Econometrica, 49, 1057-1072.
- 387 Elliot, G., Rothenberg, T.J. and Stock, J.H. (1996). Efficient tests for an autoregressive unit root.
 388 Econometrica, 64, 813-836.
- 389 Folland, C.K., Colman, A.W., Smith, D.W., Boucher, O., Parker, D.E. and Vernier, J-P. (2013). High
 390 predictive skill of global surface temperature a year head. Geophysical Research Letters, 40(4), 761-
 391 767.
- 392
- 393 Geweke, J. (1982). Measurement of linear dependence and feedback between multiple time series.
 394 Journal of the American Statistical Association, 77, 304-324.
- 395
- 396 Ghodsi, M., Hassani, H. and Sanei, S. (2010). Extracting fetal heart signal from noisy maternal ECG
 397 by singular spectrum analysis. Journal of Statistics and its Interface, Special Issue on the Application
 398 of SSA, 3(3), 399-411.
- 399
- 400 Gil-Alana, L.A., Yaya, O.S., and Shittu, O.I. (2014). Global temperatures and sunspot numbers. Are
 401 they related? Physica A: Statistical Mechanics and its Applications, 396(15), 42-50.
- 402
- 403 Granger C.W.J. (1969). Investigating causal relations by econometric models and cross-spectral
 404 methods. Econometrica, 37, 424-439.
- 405
- 406 Gray, L.J., Beer, J., Geller, M., Haigh, J.D., Lockwood, M., Matthes, K., Cubasch, U., Fleitmann,
 407 D., Harrison, G., Hood, L., Luterbacher, J., Meehl, G.A., Shindell, D., van Geel, B. and White, W.
 408 (2010). Solar influences on climate. Review of Geophysics, 48(4). DOI: 10.1029/2009RG000282.
- 409
- 410 Gupta, R., Gil-Alana, L. And Yaya, O. (2015). Does sunspot numbers cause global temperatures?
 411 Evidence from a frequency domain causality test. *Applied Economics*, 47 (8), 798-808.
- 412
- 413 Hassani, H. (2007). Singular spectrum analysis: methodology and comparison. Journal of Data
 414 Science, 5, 239-257.
- 415

- 416 Hassani, H., Heravi, S. and Zhigljavsky, A. (2009). Forecasting European industrial production with
417 singular spectrum analysis. *International journal of forecasting*, 25(1), 103-118.
418
- 419 Hassani H. and Thomakos, D. (2010). A review on singular spectrum analysis for economic and
420 financial time series. *Statistics and its Interface*, 3, 377-397.
421
- 422 Hassani H., Zhigljavsky, A., Patterson, K., et al. (2010). A comprehensive causality test based on the
423 singular spectrum analysis. *Causality in Science*, 379-406.
424
- 425 Hassani H., Soofi A. S. and Zhigljavsky, A. (2013a). Predicting inflation dynamics with singular
426 spectrum analysis. *Journal of the Royal Statistical Society: Series A (Statistics in Society)*, 176(3),
427 743-760.
- 428 Hassani, H., Heravi, S. and Zhigljavsky, A. (2013b), Forecasting UK Industrial Production with
429 Multivariate Singular Spectrum Analysis. *Journal of Forecasting*, 32, 395–408.
- 430 Hassani, H. and Mahmoudvand, R. (2013). Multivariate singular spectrum analysis: A general view
431 and new vector forecasting approach. *International Journal of Energy and Statistics*, 1, 55-83.
432
- 433 Hassani, H. Silva, E. S., Gupta, R., and Das, S. (2015). Predicting Global Temperature Anomaly: A
434 Definitive Investigation Using an Ensemble of Twelve Competing Forecasting Models. Department
435 of Economics, University of Pretoria, Working Paper No. 201561.
436
- 437 Holmes, J.M., and Hutton, P.A. (1990). On the Casual Relationship between Government
438 Expenditures and National Income. *The Review of Economics and Statistics*, 72(1), 87-95.
439
- 440 Hosoya, Y. (1991). The decomposition and measurement of the interdependence between second-
441 order stationary processes. *Probability Theory and Related Fields*, 88, 429-444.
442
- 443 Kwiatkowski, D.P., Phillips, C.B., Schmidt, P. and Shin, Y. (1992). Testing the Null Hypothesis of
444 Stationarity against the Alternative of a Unit Root. *Journal of Econometrics*, 54, 159-178.
445
- 446 Lean, J.L. and Rind, D.H. (1998). Climate forcing by changing solar radiation. *Journal of Climate*
447 11(12), 3069-3094.
448
- 449 Lean, J.L. and Rind, D.H. (2009). How will earth's surface temperature change in future decades?
450 *Geophysical Research Letters*, 36(15). DOI: 10.1029/2009GL038932.
451
- 452 Love, J.J., Mursula, K., Tsai, V.C. and Perkins, D.M. (2011). Are secular correlations between
453 sunspots, geomagnetic activity, and global temperature significant? *Geophysic Research Letters*, 38,
454 1-6.
455
- 456 Ng, S. and Perron, P. (2001). Lag length selection and the construction of unit root tests with good
457 size and power. *Econometrica*, 69, 1519-1554.
458
- 459 Phillips, P.C.B. and Perron, P. (1988). Testing for a unit root in time series regression. *Biometrika*
460 75, 335-346.
461

- 462 Pittock, B. (1978). A critical look at long term sun-weather relationships. *Review of Geophysics and*
463 *Space Physics*, 16(3), 400-420.
- 464
- 465 Pittock, B. (1983). Solar variability, weather and climate: an update. *Quarterly Journal of the Royal*
466 *Meteorological Society*, 109, 23-55.
- 467
- 468 Pittock, B. (2009). Can solar variations explain variations in Earth's climate? *Climate Change*, 96,
469 483-487.
- 470
- 471 Sanei, S. and Hassani, H. (2015). *Singular spectrum analysis of biomedical signals [M]*. CRC Press.
- 472
- 473 Scafetta, N. (2009). Empirical analysis of the solar contribution to global mean air surface
474 temperature change. *Journal of Atmospheric and Solar-Terrestrial Physics*, 71, 1916-1923.
- 475
- 476 Scafetta, N. (2011). A shared frequency set between the historical mid-latitude aurora records and
477 the global surface temperature. *Journal of Atmospheric and Solar-Terrestrial Physics*, 102, 368-371.
- 478 Scafetta N., Grigolini, P. Imholt, T., Roberts, J.A. and West, B.J. (2004). Solar turbulence in earth's
479 global and regional temperature anomalies. *Physical Review E*, 69, 026303.
- 480
- 481 Scafetta, N., and West, B.J. (2003). Solar flare intermittency and the earth temperature anomalies.
482 *Physical Review Letters*, 90, 248701.
- 483
- 484 Scafetta, N. and West, B.J. (2005). *Estimated solar contribution to the global surface warming using*
485 *the ACRIM TSI satellite composite*. *Geophysical Research Letters*, 32, L18713.
- 486
- 487 Scafetta, N. (2014), Global temperatures and sunspot numbers. Are they related? Yes, but non
488 linearly. A reply to Gil-Alana et al. (2014), *Physica A: Statistical Mechanics and its Applications*,
489 413, 329-342.
- 490 Usoskin, I.G., Schussler, M., Solanki, S.K. and Mursula, K. (2004). Solar activity over the last 1150
491 years. Does it correlate with climate? *Proceedings of 13th Cool Stars Workshop, Hamburg*.
- 492 Zhou, J. and Tung, K-K. (2013). Deducing Multidecadal Anthropogenic Global Warming Trends
493 Using Multiple Regression Analysis. *Journal of Atmospheric Science*, 70, 3-8.
- 494
- 495

Appendix

496
497498 **The Frequency Domain Causality Test**

499

500 Breitung and Candelon' (2006) presented that in a two-dimensional vector of time series $Z_t = (X_t, Y_t)$ 501 observed at time $t = 1, \dots, T$, where Z_t is a finite-order VAR process, is of the form:

502
$$\Theta(B)Z_t = \varepsilon_t, \quad t = 1, 2, \dots, \quad (A1)$$

503 where $\Theta(B) = 1 - \theta_1 B - \dots - \theta_p B^p$ is a 2×2 lag polynomial with $B^k Z_t = Z_{t-k}$. The error vector ε_t is a504 white noise process, with $E(\varepsilon_t) = 0$ and $E(\varepsilon_t \varepsilon_t') = \Sigma$, where Σ is a positive definite variance matrix.505 The VAR process may include a constant, a trend or dummy variables. The matrix Σ is then506 decomposed as $G'G = \Sigma^{-1}$ where G is the lower triangular matrix of the Cholesky decomposition.

507 With the assumption that the system is stationary, the moving average (MA) representation of the

508 process is,

509
$$Z_t = \Phi(B)\varepsilon_t = \begin{pmatrix} \phi_{11}(B) & \phi_{12}(B) \\ \phi_{21}(B) & \phi_{22}(B) \end{pmatrix} \begin{pmatrix} \varepsilon_{1t} \\ \varepsilon_{2t} \end{pmatrix} = \begin{pmatrix} \psi_{11}(B) & \psi_{12}(B) \\ \psi_{21}(B) & \psi_{22}(B) \end{pmatrix} \begin{pmatrix} \xi_{1t} \\ \xi_{2t} \end{pmatrix} = \Psi(B)\xi_t \quad (A2)$$

510 where $\Psi(B) = \Phi(B)G^{-1}$. Then, the spectral density of X_t can be expressed as:

511
$$f_x(\omega) = \frac{1}{2\pi} \left[\left| \psi_{11}(e^{-i\omega}) \right|^2 + \left| \psi_{12}(e^{-i\omega}) \right|^2 \right]. \quad (A3)$$

512 Using the following measure of causality, as in Geweke (1982) and Hosoya (1991):

513
$$M_{Y \rightarrow X}(\omega) = \log \left[1 + \frac{2\pi f_x(\omega)}{\left| \psi_{11}(e^{-i\omega}) \right|^2} \right]. \quad (A4)$$

514 Replacing (A3) into (A4) gives,

$$M_{Y \rightarrow X}(\omega) = \log \left[1 + \frac{|\psi_{12}(e^{-i\omega})|^2}{|\psi_{11}(e^{-i\omega})|^2} \right]. \quad (A5)$$

Note that, Equation (A5) is zero, if $|\psi_{12}(e^{-i\omega})|^2 = 0$, which implies that Y does not Granger-cause X at frequency ω .

The null hypothesis that Y does not Granger-cause X at frequency ω is then given as:

$$H_0: M_{Y \rightarrow X}(\omega) = 0. \quad (A6)$$

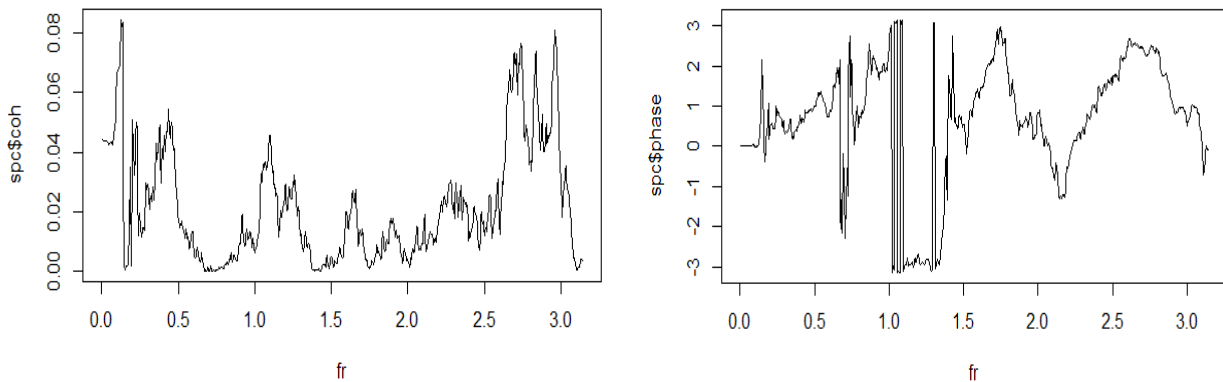
The statistic $M_{Y \rightarrow X}(\omega)$ is then obtained by replacing $|\psi_{11}(e^{-i\omega})|$ and $|\psi_{12}(e^{-i\omega})|$ in (A5) by the estimated values obtained from the fitted VAR.

Cross Spectrum Analysis

For the total sample and all subsamples, we performed the cross spectrum analysis on SS and GT, as well as on SS and detrended GT series for comparison. Briefly, the cross spectrum analysis is the Fourier transformation of cross-covariance of two series, which gives us the degree of relationship between two series at different frequency. For each case, i.e., SS and GT and SS and detrended GT, while conducting the cross spectrum analysis, two types of figures are provided: the squared coherency by frequency and the phase spectrum by frequency. If the squared coherency is large at some specific frequencies, it implies that we can probably consider linear relationship between two tested series at these frequencies. Therefore, we then refer to the figure of the phase spectrum by frequency at these frequencies with relatively large squared coherency. If the phase spectrum is approximately linear with a positive slope, it will suggest the first variable lead changes in the duration of the second variable. When we change the order of variables in the beginning, the final results will be identical for the squared coherency, but an opposite slope should emerge for the phase

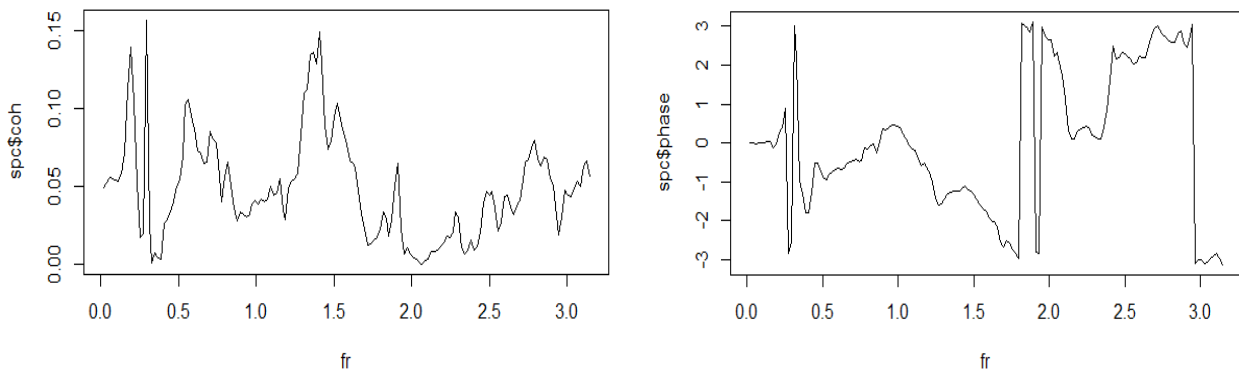
537 spectrum accordingly. Here we only provide the results where sunspots numbers is the first variable.
538 As can be seen from the results below, we can generally conclude that, unlike the SSA-based
539 approach, there is not much clear-cut evidence of SS causing GT based on the cross-spectrum
540 analysis.

541 **Total Sample (original series)**



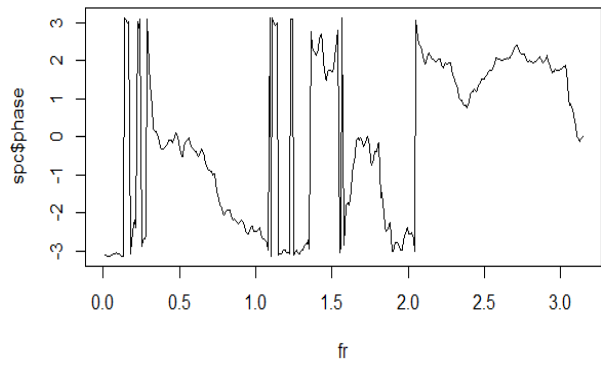
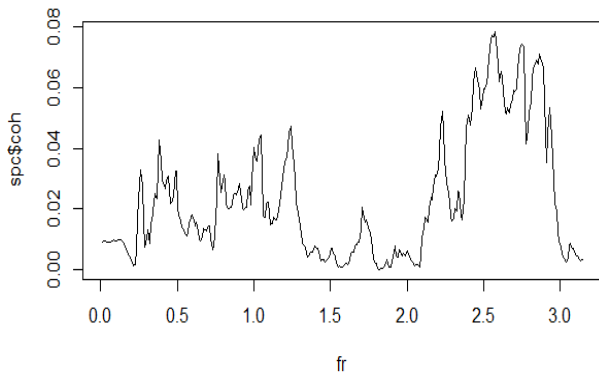
542

543 **Total Sample (detrended series)**

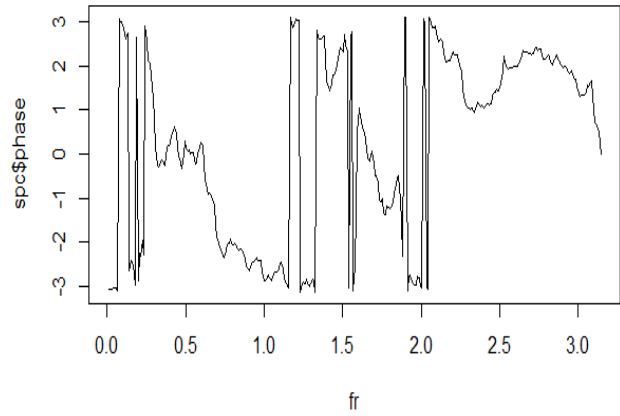
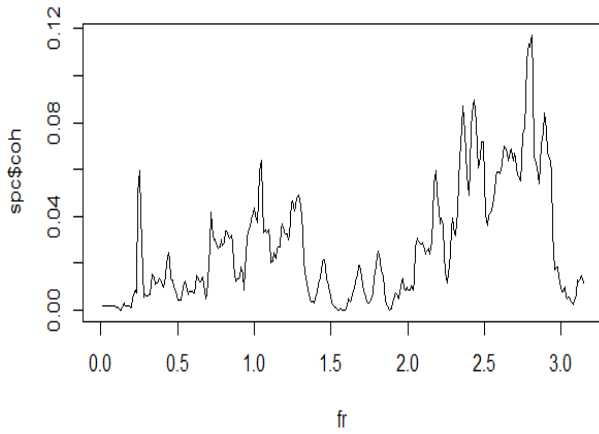


544

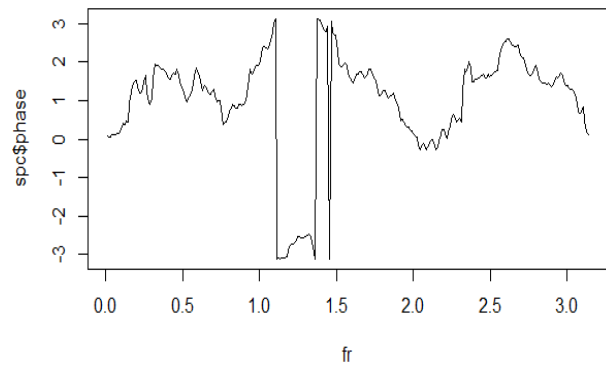
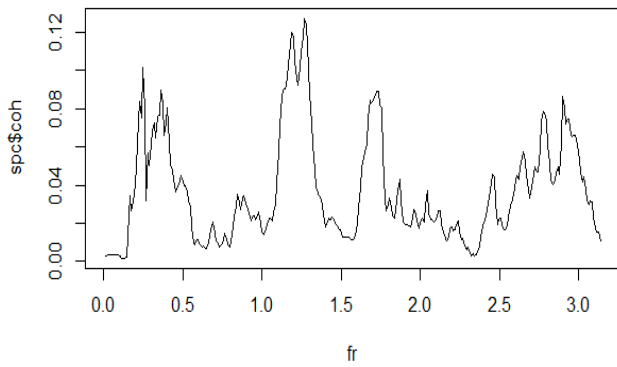
545 **Subsample A (original series)**



546

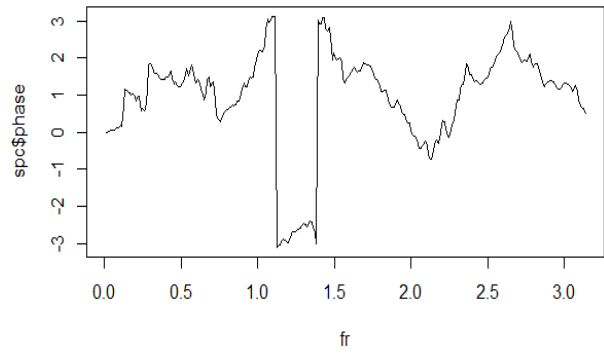
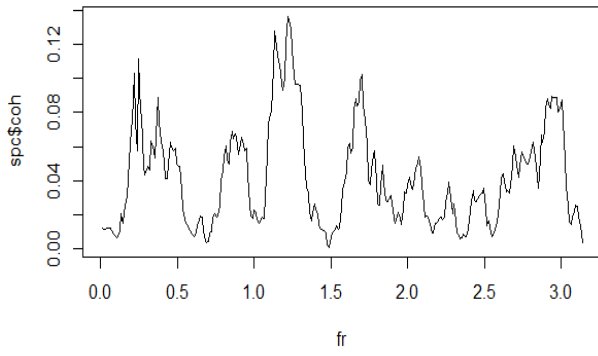
547 **Subsample A (detrended series)**

548

549 **Subsample B (original series)**

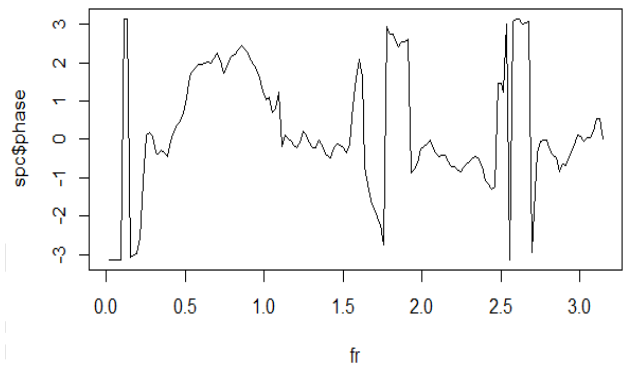
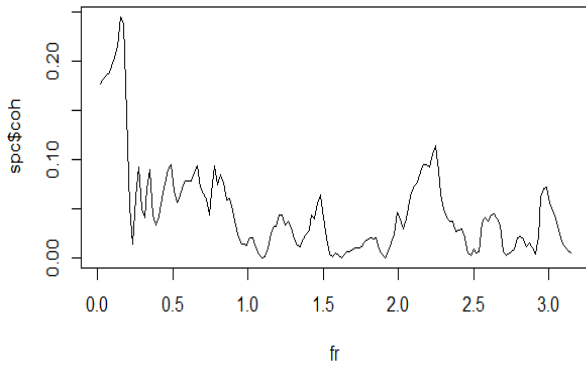
550

551 **Subsample B (detrended series)**



552
553

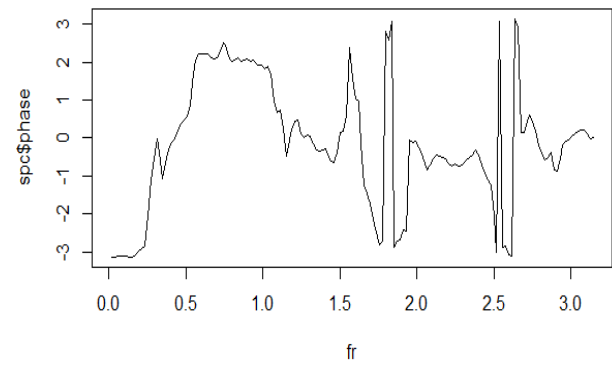
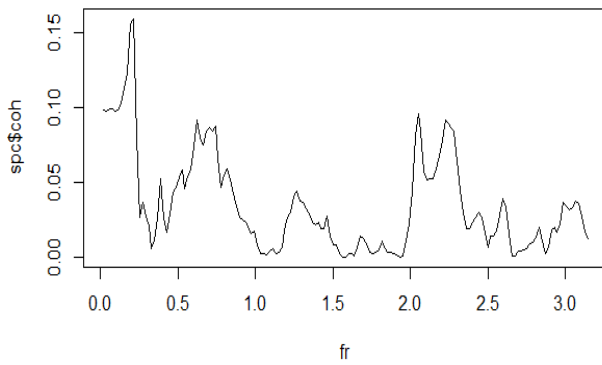
Subsample C (original series)



554

555

Subsample C (detrended series)



556